ACS APPLIED MATERIALS & INTERFACES

Research Article

www.acsami.org

Aminosilane-Grafted Polymer/Silica Hollow Fiber Adsorbents for CO_2 Capture from Flue Gas

Fateme Rezaei,[†] Ryan P. Lively,[‡] Ying Labreche,[†] Grace Chen,[†] Yanfang Fan,[†] William J. Koros,*[,†] and Christopher W. Jones*[,†]

[†]School of Chemical & Biomolecular Engineering, Georgia Institute of Technology, 311 Ferst Drive, Atlanta, Georgia 30332, United States

[‡]Algenol Biofuels, 28100 Bonita Grande Drive, Bonita Springs, Florida 34315, United States

ABSTRACT: Amine/silica/polymer composite hollow fiber adsorbents are produced using a novel reactive post-spinning infusion technique, and the obtained fibers are shown to capture CO_2 from simulated flue gas. The post-spinning infusion technique allows for functionalization of polymer/silica hollow fibers with different types of amines during the solvent exchange step after fiber spinning. The post-spinning infusion of 3-aminopropyltrimethoxysilane (APS) into mesoporous silica/cellulose acetate hollow fibers is demonstrated here, and the materials are compared with hollow fibers infused with poly(ethyleneimine) (PEI). This approach results in silica/polymer composite fibers with good amine distribution and accessibility, as well as adequate porosity retained within the fibers to facilitate rapid mass transfer and adsorption kinetics. The CO_2 adsorption capacities for the APS-infused hollow fibers are shown to be comparable to those of amine powders with similar amine loadings. In contrast, fibers that are spun with presynthesized, amine-loaded mesoporous silica powders show negligible CO_2 uptake and low amine loadings because of loss of amines from the silica materials during the fiber spinning process. Aminosilica powders are shown to be more hydrophilic than the corresponding amine containing composite hollow fibers, the bare polymer as well as silica support. Both the PEI-infused and APS-infused fibers demonstrate reduced CO_2 adsorption upon elevating the temperature from 35 to 80 °C, in accordance with thermodynamics, whereas PEI-infused powders show increased CO_2 uptake over that temperature range because of competing diffusional and thermodynamic effects. The CO_2 adsorption kinetics as probed via TGA show that the APS-infused hollow fiber adsorbents have more rapid uptake kinetics than their aminosilica powder analogues. The adsorption performance of the functionalized hollow fibers is also assessed in CO_2 breakthrough experiments. The breakthrough results show a sharp CO_2 front for APS-grafted fibers, indicating fast kinetics with comparable pseudo-equilibrium capacities to the CO_2 equilibrium capacities measured via thermogravimetric analysis (TGA). The results indicate the post-spinning infusion method provides a new platform for synthesizing composite polymer/silica/amine fibers that may facilitate the ultimate scale-up of practical fiber adsorbents for flue gas CO_2 capture applications.

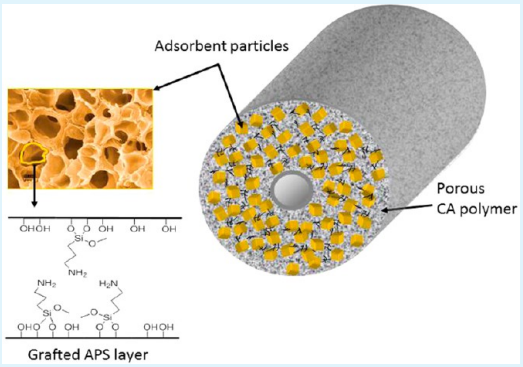

KEYWORDS: *hollow fiber adsorbents, solid-supported amines, APS, CO_2 capture, adsorption, RTSA*

1. INTRODUCTION

The concentration of CO_2 in the atmosphere continues to increase at an accelerating rate because of anthropogenic emissions, and the increasing global atmospheric CO_2 concentration has been linked to global climate change.[1] Over the past decade, numerous efforts have been devoted to mitigate this change by capturing CO_2 from major source points such as coal or gas-fired power plants.[2−4] Despite such efforts, a scalable and cost-effective technology is still lacking. Among various capture technologies, CO_2 chemical absorption by aqueous amine solutions remains, in many cases, the most viable and practical way for reducing CO_2 emissions.[5,6] However, this process is quite energy intensive, resulting in an increase in parasitic load on the plant and hence the final cost of electricity to the consumer.

Conventional swing adsorption processes such as pressure- or temperature-swing adsorption (PSA/TSA) have been widely considered for post-combustion capture; however, these processes are not energy-efficient, and the cost related to pressurizing the flue gas in the case of PSA or long regeneration time in the case of TSA may limit their use in large-scale post-combustion CO_2 capture.[7] Therefore, a potentially low-cost carbon capture system that could be retrofitted onto existing power plants is still needed.

Recently, Lively et al. have demonstrated a new carbon capture system based on a novel hollow fiber-based solid adsorbent operating in rapid TSA mode that avoids many

Received: February 19, 2013
Accepted: March 29, 2013
Published: March 29, 2013

deficiencies associated with conventional cyclic sorption processes.[8−10] This strategy is based on embedding solid adsorbent particles in a porous polymeric hollow fiber matrix for use in a rapid TSA system. In this approach, polymeric hollow fibers similar to those already prepared on commercial scales for membrane gas separations are prepared and loaded with large volumes of solid CO_2 adsorbing materials. However, unlike traditional polymer fibers for membrane applications, these hollow fibers have several unique aspects to their design. First, very high volumes of adsorbent materials are included, typically 60−70% by volume. Second, the polymeric phase is designed to have many large voids, allowing rapid mass transfer to the adsorbent particles. Third, a dense lumen layer is installed in the fiber bore to largely shut down transport from the shell side of the fibers to the bore (stopping exactly the transport that occurs in membrane applications).[11]

This design yields fibrous structures that are ideally suited for application as combined sorption and heat transfer modules in a rapid temperature swing adsorption (RTSA) process. It is recognized that zeolite 13X (used as the "proof of concept" filler in earlier reports[8,9]) is not an effective adsorbent for post-combustion CO_2 capture from wet gas streams. In contrast, supported amine adsorbents are highly efficient CO_2 adsorbents under humid conditions.[12,13] Furthermore, these materials currently lack many demonstrated implementations in scalable, continuous processes that can cope with the large heat of adsorption of amines,[14,15] which will necessitate efficient heat integration. In this regard, the hollow fiber RTSA process is ideally suited for application of typical silica amine adsorbents, as it (i) allows for effective heat integration,[11] (ii) gives fast cycle times (expected to be on the order of 2−4 min),[8] and (iii) minimizes contact of aminosilica-adsorbents with high-temperature steam, which can degrade the adsorbent.[16] Furthermore, previous energetic analysis reveals a substantial advantage for hollow fiber sorbents as compared to liquid sorption systems, primarily associated with the ease of heat integration.[11] To this end, we propose the use of supported amine materials as the adsorbents in the hollow fiber, RTSA configuration for post-combustion CO_2 capture. Large installations would employ many modules, with the number being scaled to fit flue gas streams of different sizes. Each module is expected to contain approximately 300,000 fibers. Considering a CO_2 capture rate of 90%, ∼1700 modules are needed for a power plant with a CO_2 capture rate of 250 MMSCFD (flue gas volumetric flow rate of ∼1800 MMSCFD).

There are three classes of supported amine materials that might be used in such processes.[12,16,17] Class 1 materials are based on molecular, oligomeric, or polymeric amines impregnated into porous supports.[18] Class 2 materials are based on amines covalently grafted onto porous supports, typically using organosilanes.[19,20] Class 3 materials are based on in situ polymerization of amine-containing monomers onto porous supports.[21−24] Any of these classes of materials could be candidates for implementation in the hollow fiber configuration if presynthesized adsorbents could be easily incorporated into the polymeric fibers by direct fiber spinning. However, in our previous paper on the combination of aminosilica adsorbents and polymeric hollow fibers, we demonstrated that some presynthesized amine adsorbents may not survive the hollow fiber spinning process.[25] To circumvent this problem, in that work, we demonstrated a novel technique for preparing polymeric hollow fiber adsorbents containing class 1 amine adsorbents. In this post-spinning amine infusion method, adsorbents were synthesized by infusing poly(ethyleneimine) (PEI) into polymeric hollow fibers that contained unloaded, bare porous silica particles. Hollow fibers spun using commercial cellulose acetate (CA) and mesoporous silica were infused with an amine solution after fiber spinning, during the hollow fiber formation solvent exchange step. The post-infused fiber adsorbents exhibited a CO_2 equilibrium capacity of 1.2 mmol/g fiber.[25]

For these initial "proof of concept" experiments, our simulated flue gas simply contained CO_2, H_2O, and N_2, the major components present in flue gas. However, sulfur and nitrogen oxides, oxygen, and particulates are also present in flue gas, and these species can offer specific technical challenges for the separation process. Previous work has demonstrated that certain amine types have excellent O_2 resistance,[26] and most amines are oxidatively stable at low temperature and at low oxygen partial pressures, as found in flue gas. While beyond the scope of this study, the impact of SO_2, in particular, must be considered for implementation of such a solid-supported amine system. There are only a few studies addressing the impact of SO_2 on the CO_2 adsorption behavior of solid-supported amine adsorbents,[27] though the effect of coadsorption with CO_2 on these groups is still not clear.[28]

In this study, we apply a related methodology to the synthesis of class 2 aminosilica adsorbents and demonstrate the synthesis of amine-loaded polymer/silica hollow fiber adsorbents by infusing 3-aminopropyltrimethoxysilane (APS) into polymer/silica composite fibers by the post-spinning amine infusion method. The functionalized fibers are then characterized structurally, their CO_2 uptake capacities as well as CO_2 and water adsorption isotherms are measured, and the materials are tested in CO_2 breakthrough experiments in a bench scale RTSA system. Finally, a detailed comparison of the CO_2 adsorption isotherms for composite fibers and aminosilica powders based on class 1,[12] PEI materials and class 2, APS materials are presented.

2. EXPERIMENTAL SECTION

2.1. Materials. The following commercial silicas were used as received: PD09024 and ES757 (PQ Corporation), C803 (W.R. Grace). These silica supports differ in physical characteristics such as surface area, pore volume, and particle size. The physical properties of these silicas are presented in Table 2. The following chemicals used in the adsorbent synthesis and fiber spinning process were purchased from Sigma-Aldrich: Cellulose acetate (CA) (MW 50 000), *N*-methyl-2-pyrrolidone (NMP) (Reagent Plus 99%), poly(vinylpyrrolidone) (PVP) (MW 55000), methanol (ACS grade, >99.8%), toluene (ACS grade, >99.5%), poly(ethyleneimine) (PEI) (branched, MW 800). Hexane was obtained from BDH and 3-aminopropyltrimethoxy silane (APS) was purchased from Gelest. Specialty gases were purchased as a certified grade mixture from Airgas including the following: 0.5%, 0.1%, and 10.0% CO_2 in helium. Inert UHP gases such as helium and nitrogen were also purchased from Airgas.

2.2. Aminosilica Adsorbents. Two well-established supported amine adsorbents, one based on PEI-impregnated silica (class 1) and one based on APS-functionalized silica (class 2) were evaluated for use in post-combustion CO_2 capture conditions. In a typical synthesis of a class 1 powder adsorbent, 1 g of PEI and 20 mL of methanol were first mixed for 1 h. Subsequently, 1 g of silica dried overnight was added and stirred for an additional 12 h. The methanol solvent was later removed by a rotary evaporator (rotovap), and the resulting adsorbent was further dried under vacuum at 105 °C overnight before testing. For preparation of class 2 powder adsorbents, 70 mL of toluene and 1 g of dried silica were first mixed for 1 h and then 2 g of APS was added into the mixture. The mixture was kept under vigorous stirring for 24 h

Table 1. Dope Composition Used for Spinning of Bare Silica and Direct-Spun Fibers

material	CA %	PVP %	silica %	NMP %	water %
Silica A Fiber—Bare	9.4	3.7	14.0	64.2	8.7
Silica A Fiber—APS—Direct-Spinning	12.2	4.9	15.0	59.8	8.1
Silica B Fiber—Bare	10.6	4.2	15.5	61.5	8.2
Silica B Fiber—APS—Direct-Spinning	12.5	5.0	12.5	61.6	8.4
Silica C Fiber—Bare	10.1	4.1	13.4	64.2	8.3
Silica C Fiber—APS—Direct-Spinning	11.1	4.5	22.2	54.8	7.4

at 85 °C. The resulting adsorbent was recovered by filtration, washed sequentially with toluene, hexane, and ethanol, and then dried under vacuum at 105 °C.

2.3. Fiber Formation. A description of fiber formation is similar to our previous paper.[25] A typical spinning dope contains polymer CA, adsorbent particles, NMP (solvent), water (nonsolvent), and additives (PVP). The polymers and fillers (bare silica or class 2 adsorbents) were dried at 110 °C in a vacuum oven overnight prior to use. Bare silica or class 2 aminosilica fillers were added to 80% of the required NMP/water and sonicated using a 100 W sonication horn. The mixture was stirred and sonicated alternately for 1 h to obtain a well dispersed suspension. A "prime" dope was made from 20% polymers and 20% of the required NMP/water and was stirred for 48 h on a roller. The dispersed silica mixture and prime dope were mixed together. This mixture was stirred and sonicated alternately for 1 h, and then the rest of polymers were added and mixed with mechanical stirrer for 4 h at 50 °C to completely dissolve the polymer to form the final spin-ready dope.

The hollow fibers were formed using a nonsolvent phase inversion technique commonly referred to as "dry-jet, wet-quench spinning". Spinning dopes were coextruded with a bore fluid through a spinneret into a nonsolvent water quench bath to induce phase separation and form a porous fiber. The final polymer dope solution conditions used are listed in Table 1. Fibers were spun with bare silica particles, as well as class 2 aminosilica materials. The fibers were removed from the take-up drum by clean cuts using a sharp blade and then they were placed in a bath of deionized water for 3 days—wherein the water was changed every day—to remove residual solvent. After the third day, the fibers (approximately 75 g) were solvent exchanged by immersing in three successive aliquots (400 mL) of methanol for 20 min each. Fibers were removed from the bath and allowed to dry in a fume hood in air for 1 h, then placed in a vacuum oven and dried for 2 h at 100 °C. The complete spinning conditions are given in our previous paper.[25]

2.3.1. Direct Spinning. Initially, CA polymer was directly spun from dope solutions that included aminosilica adsorbent powders. Specifically, polymer solutions with suspended adsorbent particles and solvents, nonsolvents, and additives for tuning the phase equilibria were extruded through a die into a nonsolvent quench bath. Mass transfer in the nonsolvent bath induces phase separation and the formation of a porous fiber, thereby resulting in a continuous polymer pore network with adsorbent particles suspended in the porous polymer network.

2.3.2. Post-spinning Infusion. In this approach, dried bare hollow fibers, produced according to the procedure described above, were placed in a custom-designed, jacketed reactor (40 cm length × 3 cm diameter), then mixed with toluene and a desired amount of APS. To keep the fibers and the reaction mixture near 85 °C, a circulating bath was used to circulate the heating medium through the reactor jacket. The reaction was carried out for 24 h, and the functionalized fibers were then transferred to another glass tube (with the same size as the reactor) in which the long, functionalized fibers were recovered and washed sequentially with toluene, hexane, and ethanol and then dried under vacuum at 105 °C. The experimental setup is depicted in Figure 1.

2.4. Material Characterization. Nitrogen physisorption measurements were performed using a Micromeritics Tristar II at 77 K. Surface area and pore volume were calculated from the isotherm data using the Brunauer—Emmett—Teller (BET)[29] and Barrett—Joyner—Halenda (BJH) methods, respectively. Scanning electron microscopy (SEM, LEO 1530 (Leo Electron Microscopy, Cambridge, U.K.)) was used to evaluate the fiber adsorbent pore structure and polymer—filler interfaces. To determine the organic loading of the powder adsorbents, a Netzsch STA409PG thermogravimetric analyzer was used to combust the amine groups while measuring the change in mass of the adsorbent. Elemental analysis (EA) was used to determine the nitrogen content and subsequent amine loading of the hollow fiber adsorbents. Analyses were performed by Columbia Analytical Services (Tucson, AZ, U.S.A.).

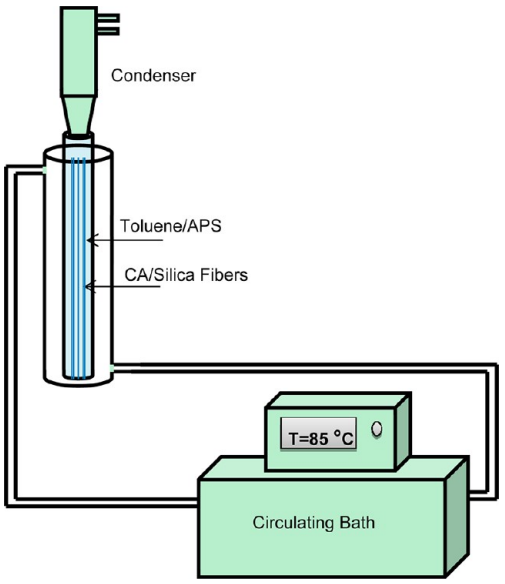

Figure 1. Layout of fiber post-spinning infusion apparatus.

2.5. Adsorption Measurements. A Q500 TGA (TA Instruments, Delaware, U.S.A.) was used to measure dry CO_2 adsorption capacities. A typical adsorption run consisted of pretreating the material for 3 h at 120 °C in flowing helium to remove preadsorbed CO_2 and water, followed by ramping down the temperature to 35 °C, the desired temperature for adsorption measurement, and then adsorbing the CO_2 gas for 5 h. The CO_2 adsorption equilibrium isotherms were constructed from data obtained using a combination of thermogravimetric analysis (TGA) at low pressure (up to 0.1 bar) and a pressure-decay cell[30] at high pressure (up to 6 bar) at constant temperatures (i.e., 35 and 80 °C). Single-component water vapor isotherms were also measured using a Hiden IGASorp (Hiden Isochema, Warrington, U.K.). A typical experiment consisted of pretreating the material at 100 °C for 10 h in flowing nitrogen, followed by cooling to 35 °C and adsorption of water vapor in flowing nitrogen gas. Adsorption was monitored at each relative humidity until a 95% equilibrium value for water adsorption capacity was reached before moving to the next data point, as determined by the equipment software.

2.6. CO_2 Breakthrough Experiments. To measure the CO_2 breakthrough capacity of post-infused fibers, 4 fibers were packed in a 20 cm long module in a 1/4″ tube with one centrally embedded thermocouple. The fiber packing fraction was 31%. A detailed description of the module and its components can be found in Lively et al.[10] The adsorption characteristics of the module were assessed in a

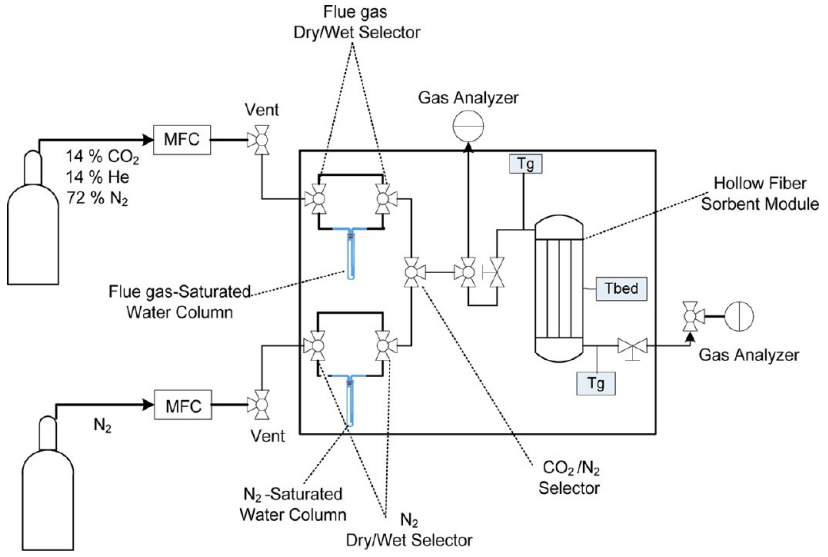

Figure 2. Process flow diagram of RTSA bench scale test station.

flow system using simulated flue gas, as shown in Figure 2. The module was degassed under flowing nitrogen at 90 °C prior to adsorption measurements. Adsorption experiments were carried out by flowing a simulated flue gas (14 mol % CO_2, 72 mol % N_2 and 14 mol % He) at 100% RH through the temperature-controlled hollow fiber adsorbent module at 40 mL/min at 35 °C and 1 atm. In this experiment, helium acted as the inert tracer, whereas nitrogen acted as the carrier gas and CO_2 was the adsorbate of interest. The concentration of CO_2 at the module outlet was transiently measured by mass spectrometry (Pfeiffer Omnistar Quadrupole mass spectrometer QMG 220) until equilibrium was reached. The moles of CO_2 adsorbed were calculated by integration of the area bounded by the CO_2 breakthrough front and the He breakthrough front from the initial concentration to the final equilibration concentration.

3. RESULTS AND DISCUSSION

3.1. Materials Characterization. For adsorbent materials in a practical CO_2 capture process, it is critical to achieve a large CO_2 capacity, fast sorption kinetics and a reasonable lifetime. The two adsorbents considered in this work for making hollow-fiber-amine adsorbent composites, a class 1 adsorbent based on PEI-impregnated into silica and a class 2 adsorbent based on APS-functionalized silica, are expected to achieve the properties mentioned above, as previous studies of these materials in powder form in our laboratory and others have demonstrated the materials to be promising.[12,31,32] Using three different commercial silica supports (i.e., ES757 as silica-A, PD09024 as silica-B, and C803 as silica-C), class 1 and class 2 powder adsorbents, as well as direct-spun and post-infused hollow fibers, were synthesized and characterized via nitrogen physisorption, EA, TGA, and scanning electron microscopy (SEM). The average particle size of the A, B, and C silicas was 25, 6.5, and 3.8 μm, respectively.

The pore volumes of the adsorbents were calculated from physisorption data using the BJH method and are presented in Table 2 and Table 3 along with the amine loading of the materials as determined by TGA and EA. The nitrogen adsorption/desorption isotherms are displayed in Figure 3. The isotherms for all the fibers are of Type IV (IUPAC classification) with hysteresis between the adsorption and the desorption branches. The data for powder adsorbents (Table 3) show that both the surface area and the pore volume of the silica supports were decreased after functionalizing them with PEI and APS.

Table 2. Physical Characteristics of Powder Adsorbent Materials

material	S_{BET} [m^2/g]	V_{Ppre} [cm^3/g]	amine loading[a] [$mmol_N/g_{SiO2}$]
Silica A−Bare	195	1.13	
Silica A−PEI	24	0.22	25.1
Silica A−APS	129	0.75	3.6
Silica B−Bare	294	1.04	
Silica B−PEI	13	0.09	22.8
Silica B−APS	50	0.21	4.6
Silica C−Bare	210	0.85	
Silica C−PEI	37	0.33	25.9
Silica C−APS	119	0.74	4.8

[a]Amine loadings determined by TGA.

In the case of fibers, it can be seen from the data in Table 3 that the surface area and pore volume decreased for all three fibers that were post-infused with APS and remained almost unchanged for fiber materials spun directly with CA polymer. This indicates that direct-spun fibers contained essentially no amines, whereas APS-derived amine moieties were most likely incorporated into the supported silicas within the polymer matrix in the case of the post-spinning infused fibers. In our previous work, we demonstrated that the adsorbent dispersion process, whereby polymer dopes were made by dispersing the adsorbent particles in an NMP solution containing dissolved polymer via sonication and solvent exchange with water after fiber formation, resulted in loss of PEI from class 1 silica adsorbents.[25] This observation necessitated the introduction of the post-spinning amine infusion process introduced in that work and applied here. Apparently, the fiber spinning process using presynthesized, APS-derived class 2 adsorbents also results in loss of amines from the silica materials, despite the presence of covalent bonds linking the amines to the supports in the as-synthesized powders.

The amine loss from the silica and/or hollow fibers during direct spinning can be attributed to the hydrolysis of the bonds between APS and the support(s) with water that is present in the dope solution.[33] To test the hydrolytic stability of the

Table 3. Physical Characteristics of Hollow Fiber Adsorbents

material	S_{BET} [m^2/g]	V_{Pore} [cm^3/g]	amine loading[a] [$mmol_N/g_{SiO2}$]
Silica A Fiber–Bare	195	0.94	
Silica A Fiber–APS–Direct-Spinning	162	0.77	1.3
Silica A Fiber–APS–Post-Spinning-Infusion	63	0. 30	8.2[b]
Silica B Fiber–Bare	221	0.60	
Silica B Fiber–APS–Direct-Spinning	179	0.55	1.4
Silica B Fiber–APS–Post-Spinning-Infusion	41	0.15	5.8[b]
Silica C Fiber–Bare	180	0.86	
Silica C Fiber–APS–Direct-Spinning	140	0.67	1.1
Silica C Fiber–APS–Post-Spinning-Infusion	57	0.28	5.9[b]

[a]Amine loadings determined by EA. [b]Amine loadings are normalized per g of silica for consistency, but this does not imply all amines are only contained within silica domains.

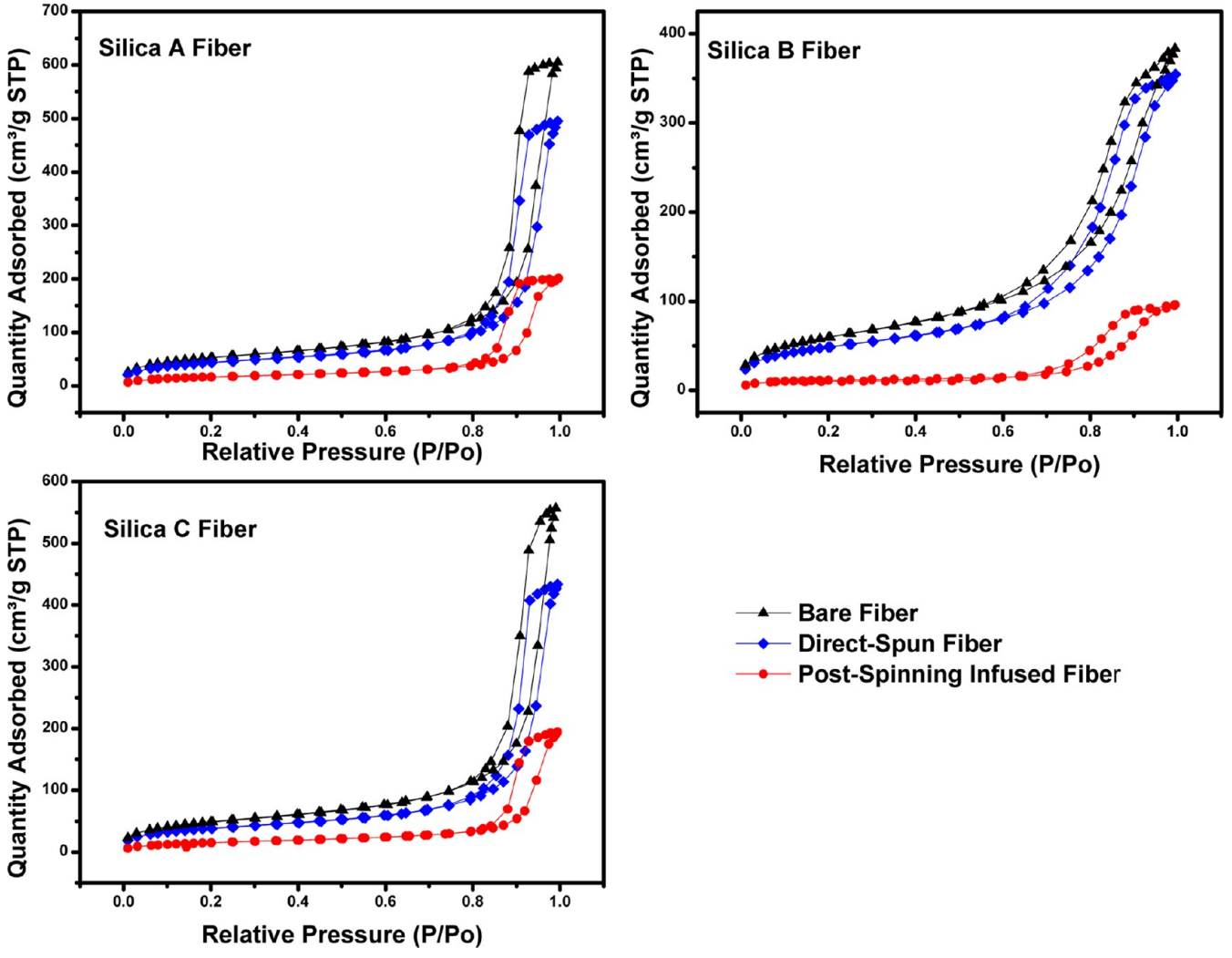

Figure 3. Nitrogen adsorption/desorption isotherms of bare, direct-spun, and post-spinning infused fibers with APS (cm^3/g fiber).

functionalized silica adsorbents, class 2 powder materials (with silica C as the support) were immersed in deionized water at ambient temperature and 50 °C for 24 h. The samples were then rinsed with water and dried at 110 °C before characterization. The amine loading was observed to drop dramatically from 3.5 to 1.5 mmol N/g at both temperatures after 24 h. These results support the hypothesis that the self-catalyzed[34] amine hydrolysis in the presence of water is likely responsible for amine loss during fiber spinning. Efforts however are underway to better identify in which step amine leaching occurs during direct spinning process.

Figure 4 shows SEM images of bare fibers as well as post-spinning infused fibers. From the images, it can be seen that all the fibers are highly porous. The silica-A particles were found to be too large for practical use in the fiber adsorbent, whereas the silica-B and -C materials were more suitable, demonstrating uniform dispersion of silica particles in the fiber. For all three fibers, the fiber wall thickness was approximated to be 300–400 μm. These micrographs qualitatively show that the fiber pore

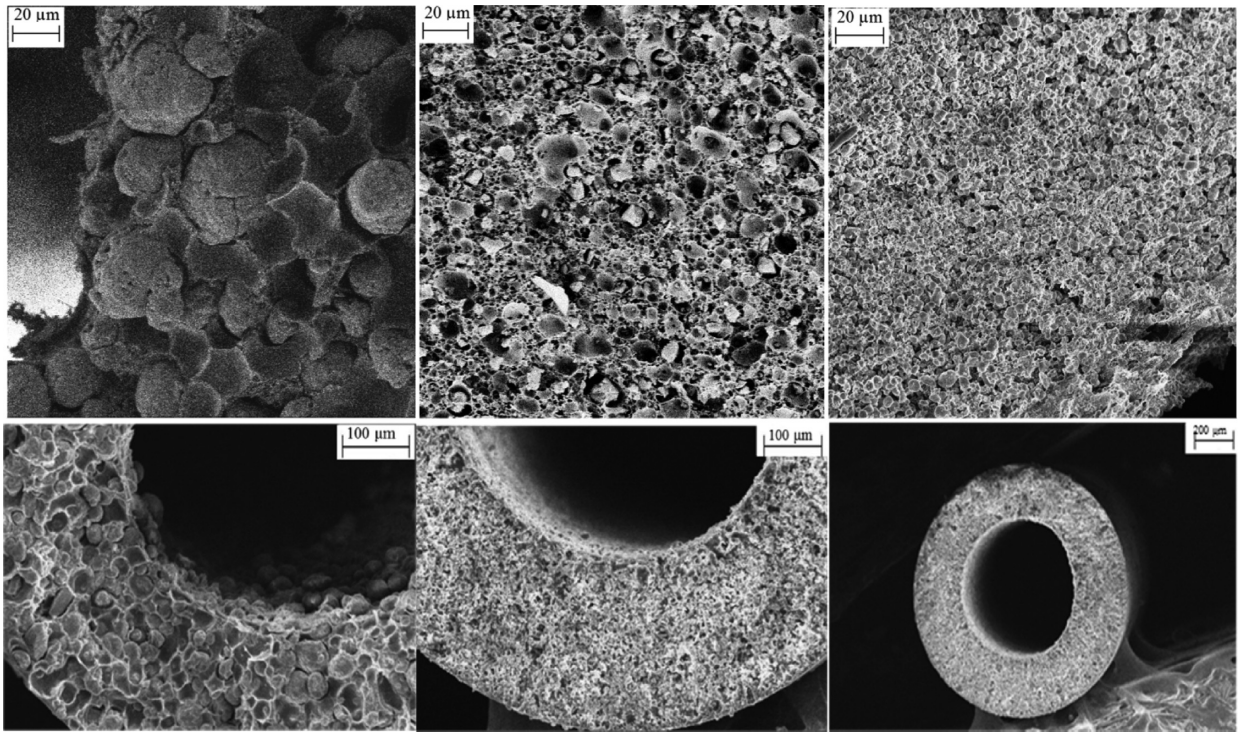

Figure 4. (top): SEM images of bare fibers, from left to right: silica-A, silica-B, and silica-C. (bottom): post-spinning infused fibers with APS, from left to right: silica-A, silica-B, and silica-C.

morphology did not collapse during processing, and a highly porous state was maintained, consistent with the nitrogen physisorption isotherms.

To further investigate the hollow fiber pore morphology after post-spinning infusion with APS, helium permeation measurements were performed on both the bare silica fibers and the post-spinning infused fibers prepared using the three different silica materials. The permeation pressure was set to 25 psig and the flux through the fiber was tested at 35 °C. Table 4 lists the

Table 4. He Permeance of Fibers at 35 °C, 25 psig

fiber code	He permeance (GPU)[a]
Silica A Fiber−Bare	88,420 ± 230
Silica A Fiber−APS−Post-Spinning-Infusion	44,420 ± 760
Silica B Fiber−Bare	90,000 ± 100
Silica B Fiber−APS−Post-Spinning-Infusion	55,490 ± 580
Silica C Fiber−Bare	80,900 ± 530
Silica C Fiber−APS−Post-Spinning-Infusion	28,860 ± 830

[a] GPU = $(cm^3(STP))/(cm^2 \cdot s \cdot cmHg) \cdot 10^{-6}$

permeation results for all the fibers. Comparing the permeance of bare and post-infused fibers, it can be seen that although the permeance decreased to a large extent by the amine infusion process for all fibers, the pore network was still open, indicating that the fiber adsorbent still had sufficient porosity for adsorption applications and that the adsorption resistances from the CA polymer matrix were minimal. These helium permeance data are in agreement with SEM micrographs of the hollow fiber adsorbents shown in Figure 4, supporting the notion that the fibers are in a highly porous state in all cases.

3.2. Adsorption Measurements. *3.2.1. CO_2 Capacity of Hollow Fiber and Powder Adsorbents.* The CO_2 adsorption capacities of the aminosilica adsorbent powders as well as direct-spun and post-infused hollow fibers were measured at 10% CO_2 concentration (balance with helium) and 35 °C using a TGA. Comparing amine efficiencies of the powder and fiber adsorbents, as shown in Figure 5, it can be observed that post-

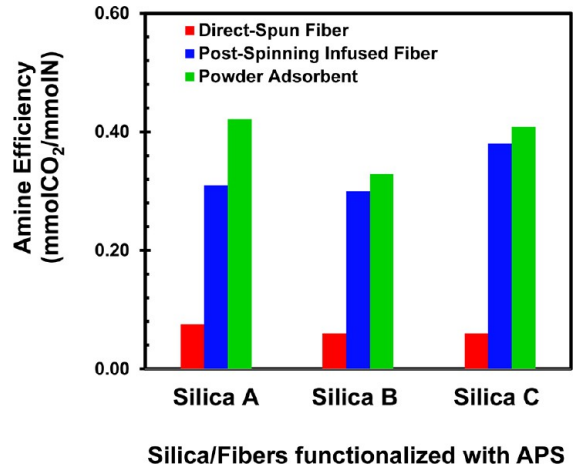

Figure 5. Amine efficiency of aminosilica powder and functionalized hollow fibers prepared using APS at 35 °C.

spun fibers showed comparable capacities to powder adsorbents, whereas direct-spun fibers exhibited essentially zero amine efficiency (mainly because of the negligible CO_2 capacity). This supports the observations described above that suggest that the combination of sonication treatment that was used to disperse the silica materials in the polymer dope solution and the solvent exchange step after spinning (when the fiber composites are soaked in a water bath) was likely responsible for amine leaching from the direct-spun fibers.

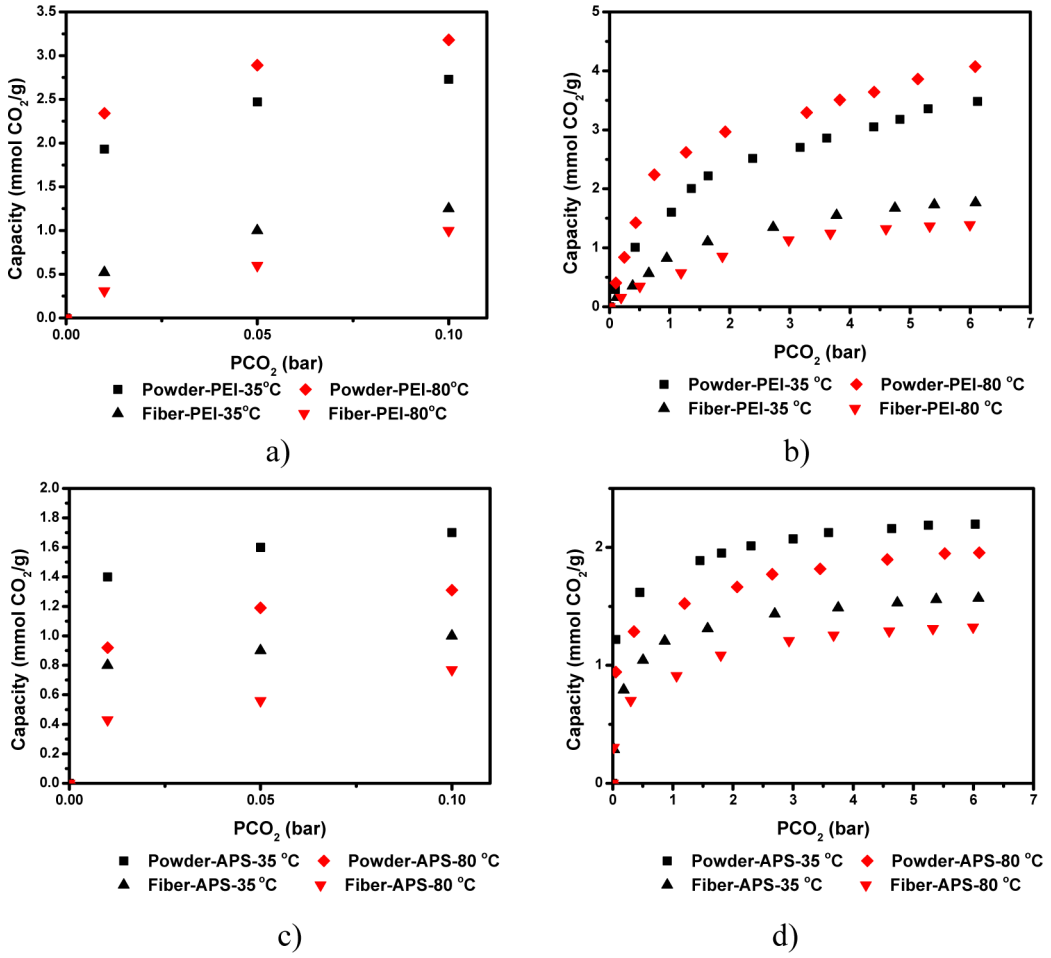

Figure 6. CO_2 adsorption isotherms for aminosilica powders and amine-functionalized hollow fibers made with silica C and (a) and (b) PEI (class 1), (c) and (d) APS (class 2) at 35 and 80 °C.

3.2.2. CO_2 Adsorption Isotherms in Hollow Fiber and Powder Adsorbents. Low-pressure adsorption isotherms were approximated by measuring dry CO_2 adsorption capacities using a TGA, while pressure decay adsorption experiments were used to study adsorption at higher pressures. The adsorption isotherms for hollow fiber and aminosilica powder adsorbents obtained at 35 and 80 °C are displayed in Figures 6a,b and 6c,d, respectively. For powders made with PEI (class 1 materials), an apparent increase in the "equilibrium" CO_2 capacity with increasing temperature was observed. This non-thermodynamic behavior has been previously observed in the literature[12,13,18,35−37] and results from significant kinetic limitations for gas diffusion within the aminopolymer-filled support materials. At low temperatures, strong binding of CO_2 within the PEI-filled pores can significantly hinder further diffusion of CO_2 through the remaining clean adsorbent, leading to depressed uptakes at low temperatures. At higher temperatures, the interaction between CO_2 and the amine is significantly reduced and the polymer chain mobility of the PEI is drastically increased, thus more of the adsorbent becomes accessible for CO_2 sorption. In contrast, the CO_2 capacity of the class 2 powder adsorbents decreased by increasing temperature as thermodynamically expected for exothermic adsorption reactions. This non-thermodynamic behavior has been observed for grafted amines similar to class 1 adsorbents in cases where the pores were blocked.[38,39] The thermodynamic behavior of class 2 materials clearly suggests that there is no such pore blockage in the APS-functionalized materials evaluated in this study.

In contrast to the results with class 1 powders, fiber adsorbents prepared using post-infusion of PEI (class 1) or APS (class 2) displayed higher capacities at lower temperatures, as would be expected based on thermodynamics. The differing behavior of the fiber and powder adsorbents can be rationalized based on the hypothesized distribution of amine groups in each material. For the PEI-containing materials, class 1 powders have their pores largely filled with PEI, and this leads to increased adsorption at temperatures up to about 70−80 °C, because of competing kinetic (diffusion) and thermodynamic (adsorption) effects. However, for class 1 fibers, the PEI is likely distributed over both the silica pores as well as throughout the CA polymer pores, and a broader distribution of amines may lead to smaller amine domain sizes and hence the absence of diffusion effects associated with large PEI domains. Similarly, in class 2 fibers, the amine sites would again be expected to be distributed in both the silica and the polymer phases, with the good distribution again leading to thermodynamic-limited adsorption behavior as a function of temperature.

3.2.3. Water Adsorption Isotherms in Hollow Fiber and Powder Adsorbents. Because of the humid nature of flue gases, assessing the role of water adsorption is important for selecting the best adsorbent for capturing CO_2 from these streams. It is well-known that hydrophilic amine materials can facilitate the adsorption of CO_2 molecules and hence exhibit high CO_2

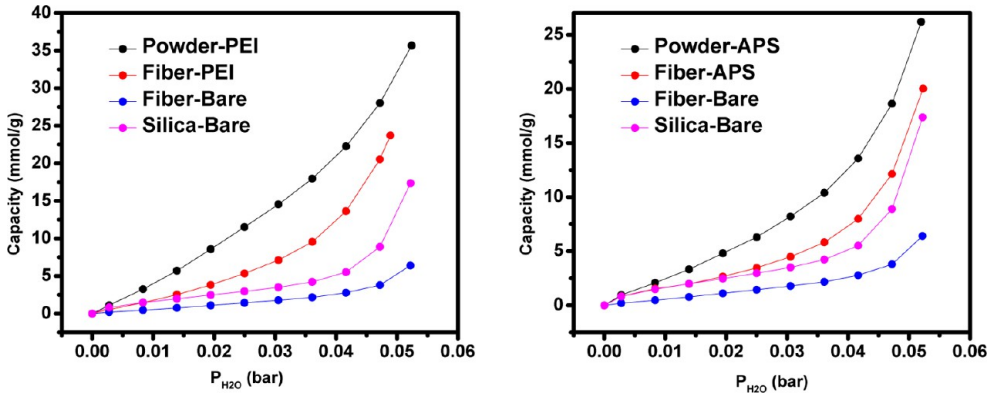

Figure 7. Water adsorption isotherms (mmol/g sample) of aminosilica powders and amine functionalized hollow fibers using silica C in (a) PEI (class 1) and (b) APS (class 2) forms at 35 °C.

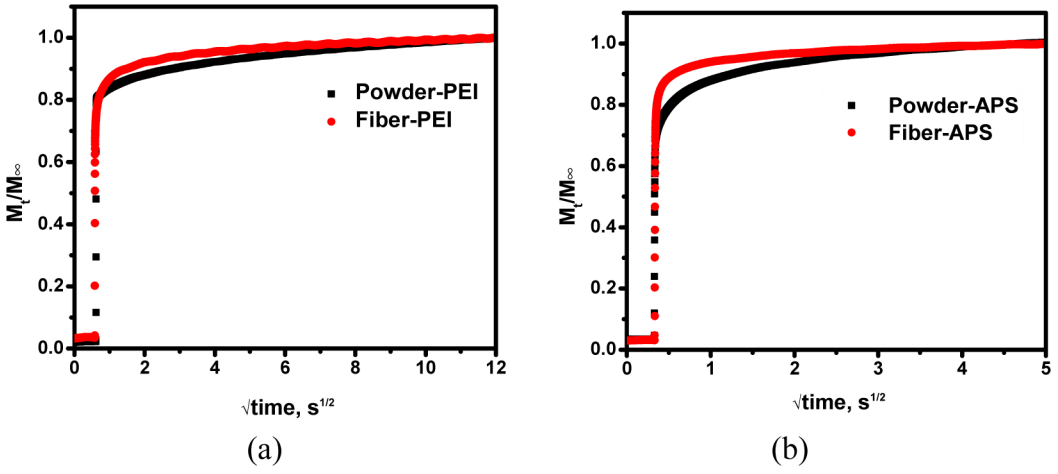

Figure 8. CO_2 uptake response time comparisons between aminosilica powders and functionalized hollow fibers with silica C and (a) PEI (class 1) and (b) APS (class 2) forms at 35 °C.

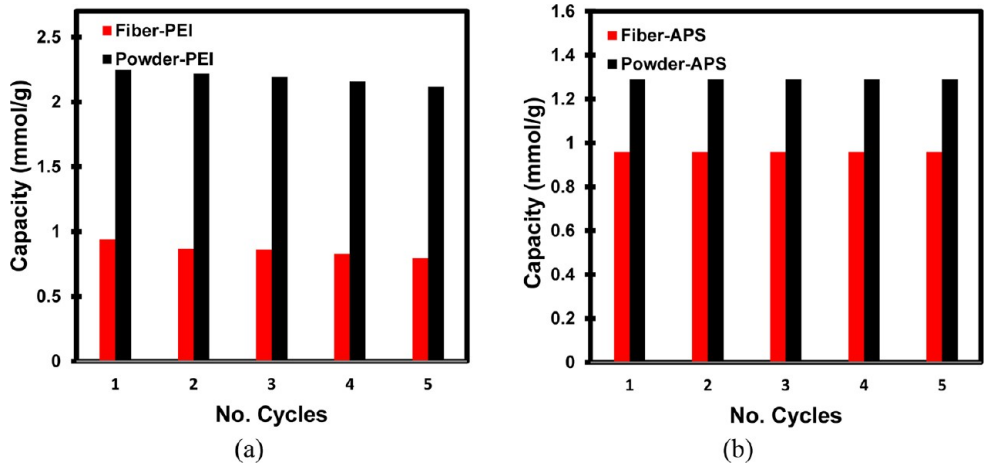

Figure 9. Thermal cycling of (a) PEI based (class 1) and (b) APS based (class 2) aminosilica powder and aminosilica fiber adsorbents made with silica C (mmol/g sample) in a 10% CO_2/He atmosphere at 35 °C.

capacity.[12] However, high hydrophilicity can result in low CO_2 adsorption capacity because of pore blockage as a result of water condensation in the pores, which hinders CO_2 access to the adsorption sites within the solid. Thus, water vapor adsorption isotherms were measured for both powder and fiber adsorbents at 35 °C, and the results are displayed in Figures 7a and 7b. As can be seen in these figures, for both class 1 and class 2 materials, the powder adsorbent displayed higher water uptake than the functionalized fiber at all relative humidities. For both cases, the water uptake of the bare silica and bare fiber were significantly lower than that of the amine functionalized materials, especially at higher relative humidities, consistent with past work on APS-modified materials.[40] In addition, the data suggest that liquid water fills the pores at higher relative

dx.doi.org/10.1021/am400636c | ACS Appl. Mater. Interfaces 2013, 5, 3921−3931

humidities; this can be verified by calculating the maximum water uptake for the bare and functionalized fibers from pore volume values. The maximum water uptakes for the silica-C bare and grafted fibers are 47 mmol/g fiber and 15.5 mmol/g fiber, respectively. Therefore, at higher unit activity water, the breakthrough testing conditions are very close to liquid-filled pores, and significant water is likely present within the pores of the APS-grafted fiber.

3.2.4. Kinetic Uptake of CO_2 in Hollow Fiber and Powder Adsorbents. TGA adsorption experiments were performed to determine adsorption times for the powder and hollow fiber adsorbents. The uptake curves for class 1 and class 2 powders along with post-spinning infused fibers are shown in Figures 8a and 8b. For both cases, the fiber adsorbents achieved greater than 95% equilibration in less than 16 s. The aminosilica powder adsorbents, however, lagged behind the fiber adsorbents in apparent response time, in part because of retarded heat dissipation in the TGA pan for the well-packed experimental powder bed as compared to the loosely packed experimental fiber bed. This may also be due to better dispersion of amines in fibers compared to powders. The uptake results show quite rapid adsorption equilibration for hollow fiber adsorbents functionalized with PEI and APS, demonstrating the fiber geometry to facilitate rapid uptake compared with powder beds. These results are in agreement with previous studies on zeolite 13X powders and fiber adsorbents embedded with zeolite 13X.[8]

3.2.5. Cyclic Thermal Performance of Hollow Fiber and Powder Adsorbents. To obtain preliminary insight into the cyclic stability of the amine-loaded hollow fiber adsorbents, cyclic TGA experiments were performed by cycling the furnace temperature between 35 and 120 °C and switching the gas between 10% CO_2/helium and pure helium in adsorption/desorption cycles. Figures 9a and 9b show the cyclic mass gain/loss versus time for five cycles, where a cycle is 500 min long. Figure 9a illustrates that the capacity of class 1 adsorbents degraded during moderate cycling. For example, the adsorption capacities of the PEI functionalized hollow fibers decreased by a factor of 0.10 after five cycles, from 1.0 to 0.90 mmol/g fiber. This result shows that the class 1 amine-impregnated adsorbent, although having a high initial adsorption capacity, may have limited stability under dry conditions. This is consistent with studies that use class 1, PEI-impregnated amine powders.[41] Furthermore, a change in baseline is observed for both infused silica and fiber adsorbents with PEI. This might be attributed to the loss of water and low molecular weight oligomers from PEI by heating the sample during desorption steps. In contrast, it can clearly be seen from Figure 9b that for class 2 materials, both powder and fiber adsorbents retained their capacities after 5 cycles and showed good regenerability and stability in cyclic operations, even using relatively high desorption temperatures. Previous studies demonstrated that the reaction between PEI and dry CO_2 can lead to urea formation, which deactivates the amine and therefore decreases capacity at elevated temperatures.[42,43] However, in a later investigation, Sayari and Belmabkhout[44] provided evidence that the presence of water vapor inhibits the formation of ureas, thereby stabilizing the amine adsorbents to CO_2 deactivation. These data suggest that the targeted RTSA operating temperature window, at 120 °C and below, along with operation using humidified gases (flue gases are naturally humidified) may allow for stable operation with the functionalized fibers with regard to urea formation. However, more extensive testing is needed on the stability and regenerability of fibers over a larger number of adsorption−desorption cycles.

3.3. CO_2 Breakthrough Experiments. Figures 10a−c show the helium, CO_2, and water breakthrough curves of a fiber

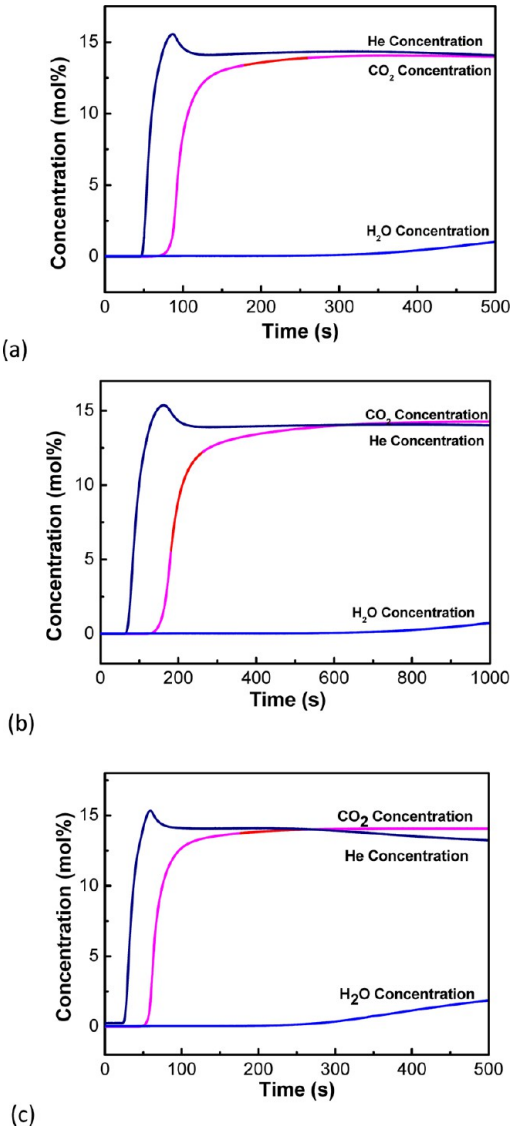

Figure 10. CO_2 breakthrough curves for post-spinning infusion, APS-functionalized fibers (class 2) using fibers containing (a) silica-A, ES757; (b) silica-B, PD09024; and (c) silica-C, C803 fibers.

module containing 4 hollow fibers functionalized with APS by the post-infusion method. Helium is used as a non-interacting tracer to capture the mean residence time of a gas in the sorption system. As can be seen from Figure 10a, silica-A fibers with amine loading of 3.1 mmol N/g fiber were found to have CO_2 breakthrough and pseudo-equilibrium capacities of 0.24 and 0.74 mmol/g fiber, respectively. The water uptake for this fiber was 0.74 mmol/g-fiber. As observed previously with zeolite 13X[9] and class 1, PEI based[25] hollow fiber adsorbents, a helium overshoot was observed due to the displacement of helium molecules filling the void space of the fiber by the moving CO_2 front, resulting in the slight increase in the He concentration observed. This helium roll-up is qualitatively indicative of good mass transfer. As shown in Figures 10b and 10c, silica-B and silica-C functionalized fibers displayed

breakthrough capacities of 0.21 and 0.24 mmol/g and pseudo-equilibrium capacities of 0.70 and 0.71 mmol/g fiber, respectively. In addition, the water uptakes for these fibers were 1.11 and 1.45 mmol/g fiber, respectively. These results are for uncooled fibers meaning that there is no water running through the bore of the fibers (which would occur under normal operation in an RTSA process).[10] As shown previously,[10] the breakthrough capacity is higher for cooled fibers than uncooled fibers and therefore, increased breakthrough capacities for cooled fibers may be expected in the future.

4. CONCLUSIONS

The post-spinning amine infusion technique was used to functionalize polymer/silica composite fibers with aminosilanes for the first time, and the resulting materials were used for post-combustion CO_2 capture experiments using simulated flue gas. Cellulose acetate fibers containing porous silica powders were spun and APS was infused into the fibers after spinning to yield adsorbents with similar adsorption capacities and improved adsorption kinetics compared to aminosilica powders with similar amine loadings. In contrast, the direct-spinning of presynthesized aminosilica adsorbent powders led to fibers with low amine loadings, as the amine species were lost from the silica supports during the spinning process.

The CO_2 adsorption capacity of both the PEI-infused and the APS-infused fibers decreased by increasing temperature from 35 to 80 °C, in accordance with thermodynamics. The kinetic study conducted by TGA demonstrated that the PEI-infused and the APS-infused hollow fiber adsorbents had more rapid uptake kinetics than their aminosilica powder analogues. Cyclic adsorption/desorption results showed that hollow fiber adsorbents derived from APS were stable and did not lose capacity over several cyclic runs, whereas, PEI derived fibers exhibited a 10% decrease in capacity over 5 adsorption cycles. The breakthrough results indicated fast kinetics for CO_2 adsorption using the APS-infused fibers.

The collected results indicate the post-spinning infusion method provides a new platform for synthesizing composite polymer/silica/amine fibers that may facilitate the ultimate scale-up of practical fiber adsorbents for flue gas CO_2 capture applications. Considering that typical flue gas streams contain acid gas impurities such as SOx and NOx, it is important to evaluate the degree of stability of aminosilica hollow fibers in the presence of these gases. Efforts are underway to address these issues.

AUTHOR INFORMATION

Corresponding Author

*E-mail: cjones@chbe.gatech.edu (C.W.J.), william.koros@chbe.gatech.edu (W.J.K.).

Notes

The authors declare no competing financial interest.

ACKNOWLEDGMENTS

The authors acknowledge the DOE-NETL under contract DE-FE0007804 for financial support. However, any opinions, findings, conclusions, or recommendations expressed herein are those of the author(s) and do not necessarily reflect the views of the DOE.

REFERENCES

(1) Davis, S. J.; Caldeira, K.; Matthews, H. D. *Science (New York, N.Y.)* **2010**, *329*, 1330−1333.
(2) Aaron, D.; Tsouris, C. *Sep. Sci. Technol.* **2005**, *40*, 321−348.
(3) Jones, C. W. *Annu. Rev. Chem. Biomol. Eng.* **2011**, *2*, 31−52.
(4) Haszeldine, R. S. *Science (New York, N.Y.)* **2009**, *325*, 1647−1652.
(5) Reynolds, A. J.; Verheyen, T. V.; Adeloju, S. B.; Meuleman, E.; Feron, P. *Environ. Sci. Technol.* **2012**, *46*, 3643−54.
(6) Rochelle, G. T. *Science (New York, N.Y.)* **2009**, *325*, 1652−4.
(7) Rezaei, F.; Webley, P. *Sep. Purif. Technol.* **2010**, *70*, 243−256.
(8) Lively, R. P.; Chance, R. R.; Kelley, B. T.; Deckman, H. W.; Drese, J. H.; Jones, C. W.; Koros, W. J. *Ind. Eng. Chem. Res.* **2009**, *48*, 7314−7324.
(9) Lively, R. P.; Leta, D. P.; DeRites, B. A.; Chance, R. R.; Koros, W. J. *Chem. Eng. J.* **2011**, *171*, 801−810.
(10) Lively, R. P.; Chance, R. R.; Mysona, J. A.; Babu, V. P.; Deckman, H. W.; Leta, D. P.; Thomann, H.; Koros, W. J. *Int. J. Greenhouse Gas Control* **2012**, *10*, 285−294.
(11) Lively, R. P.; Mysona, J. A.; Chance, R. R.; Koros, W. J. *ACS Appl. Mater. Interfaces* **2011**, *3*, 3568.
(12) Bollini, P.; Didas, S. A.; Jones, C. W. *J. Mater. Chem.* **2011**, *21*, 15100−15120.
(13) Choi, S.; Drese, J. H.; Jones, C. W. *ChemSusChem* **2009**, *2*, 796−854.
(14) Bollini, P.; Brunelli, N. A.; Didas, S. A.; Jones, C. W. *Ind. Eng. Chem. Res.* **2012**, *51*, 15145−15152.
(15) Veneman, R.; Li, Z. S.; Hogendoorn, J. A.; Kersten, S. R. A.; Brilman, D. W. F. *Chem. Eng. J.* **2012**, *207−208*, 18−26.
(16) Li, W.; Bollini, P.; Didas, S. A.; Choi, S.; Drese, J. H.; Jones, C. W. *ACS Appl. Mater. Interfaces* **2010**, *2*, 3363−3372.
(17) Goeppert, A.; Czaun, M.; Surya Prakash, G. K.; Olah, G. A. *Energy Environ. Sci.* **2012**, *5*, 7833−7853.
(18) Xu, X.; Song, C.; Andresen, J. M.; Miller, B. G.; Scaroni, A. W. *Energy Fuels* **2002**, 1463−1469.
(19) Harlick, P. J. E.; Sayari, A. *Ind. Eng. Chem. Res.* **2007**, *46*, 446−458.
(20) Franchi, R. S.; Harlick, P. J. E.; Sayari, A. *Ind. Eng. Chem. Res.* **2005**, *44*, 8007−8013.
(21) Hicks, J. C.; Drese, J. H.; Fauth, D. J.; Gray, M. L.; Qi, G. G.; Jones, C. W. *J. Am. Chem. Soc.* **2008**, *130*, 2902−2903.
(22) Liang, Z.; Fadhel, B.; Schneider, C. J.; Chaffee, A. L. *Adsorption* **2009**, *15*, 429−437.
(23) Chaikittisilp, W.; Lunn, J. D.; Shantz, D. F.; Jones, C. W. *Chem.—Eur. J.* **2011**, *17*, 10556−10561.
(24) Liang, Z.; Fadhel, B.; Schneider, C. J.; Chaffee, A. L. *Microporous Mesoporous Mater.* **2008**, *111*, 536−543.
(25) Labreche, Y.; Lively, R. P.; Rezaei, F.; Chen, G.; Jones, C. W.; Koros, W. J. *Chem. Eng. J.* **2013**, *221*, 166−175.
(26) Bollini, P.; Choi, S.; Drese, J. H.; Jones, C. W. *Energy Fuels* **2011**, *25*, 2416−2425.
(27) Khatri, R. A.; Chuang, S. S. C.; Soong, Y.; Gray, M. *Energy Fuels* **2006**, *20*, 1514−1520.
(28) Furtado, A. M. B.; Barpaga, D.; Mitchell, L. A.; Wang, Y.; Decoste, J. B.; Peterson, G. W.; Levan, M. D. *Langmuir* **2012**, *28*, 17450−17456.
(29) Sing, K. S. W.; Everett, D. H.; Haul, R. A.W.; Moscou, L.; Pierotti, R. A.; Rouquerol, J.; Siemieniewska, T. *Pure Appl. Chem.* **1985**, *57*, 603−619.
(30) Koros, W. J.; Paul, D. R. *J. Polym. Sci.* **1976**, *14*, 1903−1907.
(31) Choi, S.; Gray, M. L.; Jones, C. W. *ChemSusChem* **2011**, *4*, 628−635.
(32) Sayari, A.; Belmabkhout, Y.; Serna-Guerrero, R. *Chem. Eng. J.* **2011**, *171*, 760−774.
(33) Smith, E. A.; Chen, W. *Langmuir* **2008**, 12405−12409.
(34) Kanan, S. M.; Tze, W. T. Y.; Tripp, C. P. *Langmuir* **2002**, *18*, 6623−6627.
(35) Song, C.; Xu, X.; Andresen, J. M.; Miller, B. G.; Scaroni, A. W. *Stud. Surf. Sci. Catal.* **2004**, *153*, 411−416.

(36) Son, W.-J.; Choi, J.-S.; Ahn, W.-S. *Microporous Mesoporous Mater.* **2008**, *113*, 31−40.
(37) Yue, M. B.; Chun, Y.; Cao, Y.; Dong, X.; Zhu, J. H. *Adv. Funct. Mater.* **2006**, *16*, 1717−1722.
(38) Chaffee, A. L.; Knowles, G. P.; Liang, Z.; Zhang, J.; Xiao, P.; Webley, P. A. *Int. J. Greenhouse Gas Control* **2007**, *1*, 11−18.
(39) Bacsik, Z.; Atluri, R.; Garcia-Bennett, A. E.; Hedin, N. *Langmuir* **2010**, *26*, 10013−24.
(40) Didas, S. A.; Kulkarni, A. R.; Sholl, D. S.; Jones, C. W. *ChemSusChem* **2012**, *5*, 2058−2064.
(41) Sayari, A.; Heydari-gorji, A.; Yang, Y. *J. Am. Chem. Soc.* **2012**, *134*, 13834−13842.
(42) Drage, T. C.; Arenillas, A.; Smith, K. M.; Snape, C. E. *Microporous Mesoporous Mater.* **2008**, *116*, 504−512.
(43) Sayari, A.; Belmabkhout, Y. *J. Am. Chem. Soc.* **2010**, *132*, 6312−6314.
(44) Sayari, A.; Belmabkhout, Y.; Serna-Guerrero, R. *Chem. Eng. J.* **2011**, *171*, 760−774.